



## The carbonate system in the East China Sea in winter

Wen-Chen Chou<sup>a,\*</sup>, Gwo-Ching Gong<sup>a</sup>, Chun-Mao Tseng<sup>b</sup>, David D. Sheu<sup>c</sup>, Chin-Chang Hung<sup>a</sup>,  
Lo-Ping Chang<sup>a</sup>, Li-Wen Wang<sup>d</sup>

<sup>a</sup> Institute of Marine Environmental Chemistry and Ecology, National Taiwan Ocean University, Keelung 202, Taiwan, ROC

<sup>b</sup> Institute of Oceanography, National Taiwan University, Taipei 106, Taiwan, ROC

<sup>c</sup> Institute of Marine Geology and Chemistry, National Sun Yat-Sen University, Kaohsiung 804, Taiwan, ROC

<sup>d</sup> Institute of Hydrological and Oceanic Sciences, National Central University, Taoyuan County 320, Taiwan, ROC

### ARTICLE INFO

#### Article history:

Received 3 December 2009

Received in revised form 26 August 2010

Accepted 16 September 2010

Available online 22 September 2010

#### Keywords:

CO<sub>2</sub>

East China Sea

Eutrophication

### ABSTRACT

Measurements of dissolved inorganic carbon (DIC), pH, total alkalinity (TA), and partial pressure of CO<sub>2</sub> (pCO<sub>2</sub>) were conducted at a total of 25 stations along four cross shelf transects in the East China Sea (ECS) in January 2008. Results showed that their distributions in the surface water corresponded well to the general circulation pattern in the ECS. Low DIC and pCO<sub>2</sub> and high pH were found in the warm and saline Kuroshio Current water flowing northeastward along the shelf break, whereas high DIC and pCO<sub>2</sub> and low pH were mainly observed in the cold and less saline China Coastal Current water flowing southward along the coast of Mainland China. Difference between surface water and atmospheric pCO<sub>2</sub> ( $\Delta p\text{CO}_2$ ), ranging from  $\sim 0$  to  $-111 \mu\text{atm}$ , indicated that the entire ECS shelf acted as a CO<sub>2</sub> sink during winter with an average flux of CO<sub>2</sub> of  $-13.7 \pm 5.7 \text{ (mmol C m}^{-2} \text{ day}^{-1})$ , and is consistent with previous studies. However, pCO<sub>2</sub> was negatively correlated with temperature for surface waters lower than 20 °C, in contrast to the positive correlation found in the 1990s. Moreover, the wintertime  $\Delta p\text{CO}_2$  in the inner shelf near the Changjiang River estuary has appreciably decreased since the early 1990s, suggesting a decline of CO<sub>2</sub> sequestration capacity in this region. However, the actual causes for the observed relationship between these decadal changes and the increased eutrophication over recent decades are worth further study.

© 2010 Elsevier B.V. All rights reserved.

### 1. Introduction

Extrapolating from measurements of the partial pressure of CO<sub>2</sub> (pCO<sub>2</sub>) in the East China Sea, Tsunogai et al. (1999) suggested that the global continental shelf is capable of absorbing atmospheric CO<sub>2</sub> at a rate of 1.0 Pg C yr<sup>-1</sup>. The potential importance of coastal oceans in absorbing atmospheric CO<sub>2</sub> is further supported by results from the North Sea (Thomas et al., 2004), in which a net CO<sub>2</sub> uptake rate of 0.4 Pg C yr<sup>-1</sup> was estimated. Recent syntheses of worldwide field measurements of the partial pressure of CO<sub>2</sub> (pCO<sub>2</sub>) indicate that continental shelves can absorb atmospheric CO<sub>2</sub> at rates ranging from 0.22 to 0.45 Pg C yr<sup>-1</sup> (Borges et al., 2005; Cai et al., 2006; Chen and Borges, 2009). These estimates account for approximately 16–71% of the currently estimated CO<sub>2</sub> uptake by the open ocean ( $1.4 \pm 1.0 \text{ Pg C yr}^{-1}$ ; Takahashi et al., 2009). The large uncertainty in these estimates reflects the complexity of coastal ecosystems and the need for greater spatial and temporal resolutions of carbon chemistry data to enable better quantification of the role of coastal oceans in global carbon cycling.

The pioneering work of Tsunogai et al. (1999) was based on a single cross shelf transect in the northern ECS (the PN line in Fig. 1a). Subsequent studies (see Table 1 for a summary) have greatly improved

both spatial and temporal coverage, yet the availability of CO<sub>2</sub> data in the ECS during winter, the most crucial period for CO<sub>2</sub> sequestration, still remains limited to the PN line and the inner shelf near the Changjiang River estuary (Fig. 1a). A thorough analysis of the carbon chemistry of the ECS in winter is therefore essential to contribute to the ECS regional estimate of CO<sub>2</sub> fluxes.

As the transition zone between the largest continent (Eurasia) and the biggest ocean (the Pacific), the ECS is the largest marginal sea in the northwest Pacific (area  $\sim 0.5 \times 10^6 \text{ km}^2$ ; Wong et al., 2000). The Changjiang River, the world's fourth largest river with an average annual water discharge of  $\sim 944 \text{ km}^3 \text{ yr}^{-1}$ , empties into the northwest corner of the ECS. The greatest discharge occurs in July and is about 5–6-fold greater than the lowest monthly discharge period, which occurs in January (Dai and Trenberth, 2002). Because of anthropogenic disturbance (e.g., intensive use of chemical fertilizers, the discharge of industrial and municipal waste waters and dam constructions), the dissolved inorganic nitrogen and phosphate concentrations in the Changjiang River flow increased by a factor of five between the 1960s and the end of the 1990s (Wang, 2006), and the Si:N ratio has declined significantly over recent decades (Gong et al., 2006). Elevated nutrient discharge causes eutrophication of the coastal waters, and stimulates some ecological consequences, including harmful algal blooms and hypoxia events, both of which have been increasing rapidly in frequency in the ECS since the 1990s (Li et al., 2007; Chen et al., 2007; Wei et al., 2007; Rabouille et al., 2008). Recent modeling studies

\* Corresponding author. Tel.: +886 2 2463 4517; fax: +886 2 2462 0892.  
E-mail address: [wcchou@mail.ntou.edu.tw](mailto:wcchou@mail.ntou.edu.tw) (W.-C. Chou).

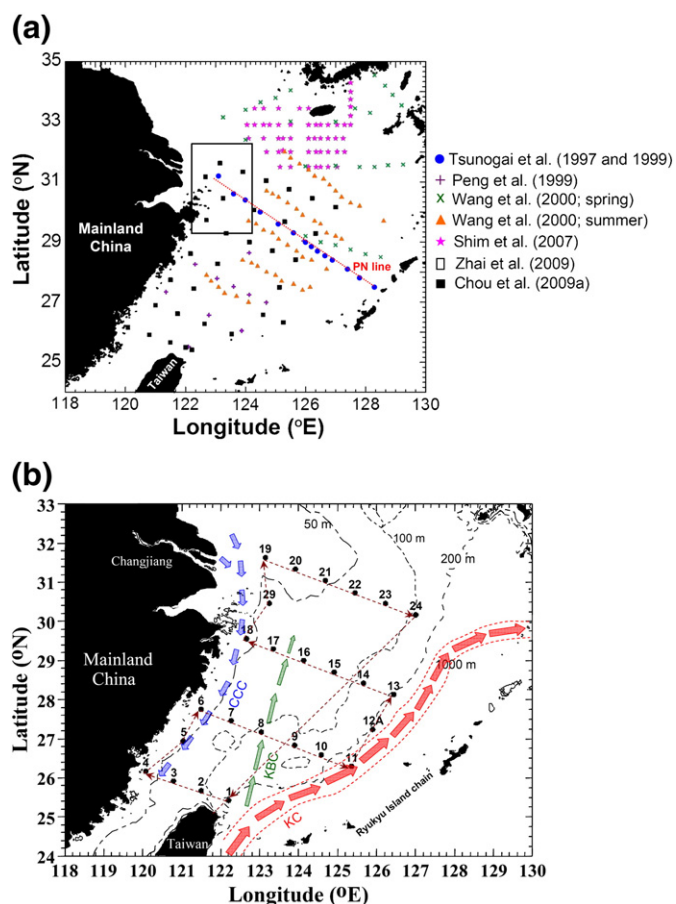


**Fig. 1.** (a) Map showing the study areas of previously published CO<sub>2</sub>-related studies in the East China Sea (ECS). It is noteworthy that the availability of CO<sub>2</sub> data in the ECS during the winter in previous studies is limited to the PN line (Tsunogai et al., 1997, 1999) and the inner shelf near the Changjiang River estuary (Zhai and Dai, 2009). (b) Bathymetric map showing the sampling locations and the cruise track for underway pCO<sub>2</sub> measurements (dashed arrows) in this study; superimposed is the schematic surface circulation system in winter, sketched from Beardsley et al. (1985). KC, Kuroshio Current; CCC, China Coastal Current; KBC, Kuroshio Branch Current.

have further suggested that eutrophication and associated changes in the N:P ratio in riverine water discharges over recent decades may have affected the capacity of the coastal areas to absorb atmospheric CO<sub>2</sub>, at both global (Mackenzie et al., 2004; da Cunha et al., 2007) and regional (Gypens et al., 2009; Borges and Gypens, 2010) scales. The impact of this eutrophication on carbonate chemistry and the sea–air CO<sub>2</sub> flux in the ECS, to the best of our knowledge, has not been thoroughly investigated to date.

We investigated the spatial distributions of dissolved inorganic carbon (DIC), pH values measured at 25 °C (henceforth, pH@25 °C), total alkalinity (TA), and pCO<sub>2</sub> in the ECS in the winter, and explored the processes that are responsible for the variations observed. Comparison of the present results with previously published datasets provided a basis for assessing the potential impact of eutrophication on carbonate chemistry in the ECS inner shelf near the Changjiang River estuary.

## 2. Methods

### 2.1. Sampling and analytical methods

A total of 25 stations along four transects in the ECS were investigated aboard the *R/V Ocean Researcher I* during 2–12 January 2008 (Fig. 1b). At each station, seawater samples were collected at six water depths (intervals of 3–25 m, depending on the bottom depth), using 20 L Niskin bottles mounted onto a rosette assembly. Water samples collected at 2 m

depth represented surface waters. Discrete subsamples for DIC, TA and pH@25 °C analyses were transferred into 350 mL pre-cleaned borosilicate bottles, and 200 μL HgCl<sub>2</sub>-saturated solution was immediately added to prevent biological alteration. Temperature and salinity were recorded using a Seabird SB9/11-plus conductivity temperature depth (CTD) system. All the hydrographic data, including temperature, salinity, DIC, TA and pH@25 °C, have been submitted to the Carbon Dioxide Information Analysis Center (CDIAC, [http://cdiac.ornl.gov/oceans/RepeatSections/repeat\\_map.html](http://cdiac.ornl.gov/oceans/RepeatSections/repeat_map.html)) for public reference.

DIC was measured using a DIC analyzer (AS-C3, Apollo SciTech Inc., Georgia, USA) (Cai and Wang, 1998). Seawater samples (0.75 mL) was acidified by addition of 0.5 mL 10% H<sub>3</sub>PO<sub>4</sub>. The extracted CO<sub>2</sub> gas was subsequently measured using a nondispersive infrared (NDIR) CO<sub>2</sub> detector (Li-COR, LI-7000) with a precision of 0.2%. At station 11 the DIC in duplicate samples was also measured using the coulometric method of Johnson et al. (1993), which had previously been used by Chou et al. (2005, 2006, 2007a,b, 2009a,b) and Sheu et al. (2009). The average difference between these two methods was  $2.4 \pm 1.4 \mu\text{mol kg}^{-1}$  ( $n=8$ ), which is within the uncertainty of DIC measurements. TA was measured (precision 0.2%) by Gran titration of a 20 mL seawater sample with 0.1 N HCl, using a Ross Orion combination electrode and precision pH meter (Orion 3-Star). For both the DIC and TA measurements certified reference material provided by A. G. Dickson (Scripps Institution of Oceanography) was used for calibration and accuracy assessments. The pH@25 °C (total hydrogen ion concentration pH scale) was determined at  $25 \pm 0.1$  °C using a Radiometer PHM-85 pH meter with a pHC2401-7 combination electrode. Buffers (2-amino-2-hydroxymethyl-1,3-propanediol and 2-aminopyridine), prepared at a salinity of 35 were used to calibrate the electrode (Dickson et al., 2007). The precision of the pH@25 °C measurements was better than  $\pm 0.005$  pH units.

During the cruise, surface temperature, salinity, and pCO<sub>2</sub> were measured continuously. Seawater from approximately 2 m depth was drawn from the vessel's moon pool. Temperature and salinity were recorded using a SBE21 SEACAT thermosalinograph system (Sea-Bird Electronics Inc.). The pCO<sub>2</sub> was determined using an underway system with continuous flow equilibration. The equilibrator used in this system was provided by the National Oceanic and Atmospheric Administration (NOAA), and is described in detail in Wanninkhof and Thoning (1993) and Feely et al. (1998). The equilibrated headspace gas was dried by passage through a water trap and a drying tube. The CO<sub>2</sub> mole fraction (xCO<sub>2</sub>) of the dried air was then detected using a NDIR spectrometer (Li-COR, LI6252), which was calibrated hourly against four gas standards (the xCO<sub>2</sub> of the four standards was 266.6, 301.8, 406.7, and 451.4 ppm) provided by the Earth System Research Laboratory, Global Monitoring Division (ESRL/GMD) of NOAA. Air was drawn from the antenna platform of the ship for the measurement of the atmospheric xCO<sub>2</sub>. The precision and accuracy of xCO<sub>2</sub> analyses were both within  $\pm 0.1$  ppm estimated by the measurements of standard gases.

### 2.2. pCO<sub>2</sub>-data reduction and internal consistency assessment

Assuming a 100% humidity of the headspace air inside the equilibrator, the water saturated pCO<sub>2</sub> (μatm) in the equilibrator (pCO<sub>2</sub><sup>(eq)</sup>) was calculated using the following formula:

$$p\text{CO}_2^{(\text{eq})} = x\text{CO}_2^{(\text{dsg})} \times [P_b^{(\text{eq})} - P_w^{(\text{eq})}],$$

where xCO<sub>2</sub><sup>(dsg)</sup> (ppm) is the measured xCO<sub>2</sub> in the dried sample gas, P<sub>b</sub><sup>(eq)</sup> (atm) is the pressure at equilibration (recorded with an onboard barometer), and P<sub>w</sub><sup>(eq)</sup> (atm) is the saturated water vapor pressure at equilibration, which was calculated using sea surface salinity (SSS) data from the surface thermosalinograph and temperature data from the temperature sensor inside the equilibrator according to the Weiss and Price (1980) formula. The pCO<sub>2</sub><sup>(eq)</sup> was then corrected to in situ

**Table 1**  
Summary of the published  $\Delta p\text{CO}_2$  ( $\mu\text{atm}$ ) and the sea–air  $\text{CO}_2$  exchange flux, and the recomputed flux ( $\text{mmol C m}^{-2} \text{ day}^{-1}$ ) in the East China Sea. The wind speed data and gas transfer algorithm used in each study are also listed. See Fig. 1a for the study areas and Section 3.3 for the details of the recomputation of flux.

Source	Study period/ (sampling time)	$\Delta p\text{CO}_2$	Wind speed data	Flux (gas transfer algorithm used)	Re-computed flux
Tsunogai et al. (1997)	Fall (Oct 1993) Winter (Feb–Mar 1993)	$-34^a/-44^b$ $-59^a/-63^b$	Not used	$-6.2^a/-8.0^b$ (A constant $\text{CO}_2$ gas exchange velocity of 3.5 $\text{m day}^{-1}$ was used.) $-10.8^a/-11.5^b$	$-6.1^a/-7.9^b$ $-5.7^a/-6.2^b$
Tsunogai et al. (1999)	Annual mean <sup>c</sup>	-55	Not used	-8.0 (A constant $\text{CO}_2$ gas exchange velocity of 2.5 $\text{m day}^{-1}$ was used.) <sup>**</sup>	-5.5
Peng et al. (1999)	Spring (May 1996)	$-28 \pm 31$	The mean wind speed observed during the cruise (8.3 $\text{m s}^{-1}$ )	-5.8 (W92S <sup>1</sup> )	-1.0
Wang et al. (2000)	Spring (Apr–May 2005) Summer (Jul 1992)	-37 -37	A constant wind speed of 7 and 6 was used for spring and summer, respectively, but data source was not indicated.	-3.2 (LM86 <sup>2</sup> ); -6.5 (T90 <sup>3</sup> ) -1.8 (LM86 <sup>2</sup> ); -4.8 (T90 <sup>3</sup> )	-2.5 -0.3
Shim et al. (2007)	Spring (May 2004) Summer (Aug 2003) Early fall (Oct 2004) Fall (Nov 2005)	$-47^d/-37^e$ $-23^d/-18^e$ $11^d/9^e$ $5^d/4^e$	Two data sources of wind speed were used: (1) in situ shipboard wind, and (2) monthly average QuikSCAT satellite wind.	(1) $-4.5 \pm 1.4$ (W92 <sup>4</sup> ); (2) $-5.0 \pm 1.6$ (W92 <sup>4</sup> ) (1) $-0.8 \pm 0.6$ (W92 <sup>4</sup> ); (2) $-2.5 \pm 1.8$ (W92 <sup>4</sup> ) (1) $1.4 \pm 2.3$ (W92 <sup>4</sup> ); (2) $1.7 \pm 2.9$ (W92 <sup>4</sup> ) (1) $0.1 \pm 0.1$ (W92 <sup>4</sup> ); (2) $0.4 \pm 0.2$ (W92 <sup>4</sup> )	$-0.5^d/-0.4^e$ $-0.1^d/-0.1^e$ $3.0^d/2.5^e$ $0.4^d/0.3^e$
Zhai and Dai (2009)	Spring <sup>f</sup> Summer <sup>f</sup> Fall <sup>f</sup> Winter <sup>f</sup> Annual mean	$-64 \pm 27$ $-60 \pm 21$ $11 \pm 45$ $-37 \pm 17$ $-41 \pm 44$	In situ shipboard wind	$-8.8 \pm 5.8$ (W92S) $-4.9 \pm 4.0$ (W92S) $2.9 \pm 2.5$ (W92S) $-10.4 \pm 2.3$ (W92S) $-5.2 \pm 3.6$ (W92S)	-1.3 -3.7 -1.1 -5.9 -2.4
Chou et al. (2009a)	Summer (Jul 2007)	$-37 \pm 78$	Daily average QuikSCAT satellite wind	$-6.3 \pm 3.1$ (W92S)	-1.4
This study	Winter (Jan 2008)	$-46 \pm 19$	Monthly average QuikSCAT satellite wind	$-13.7 \pm 5.3$ (W92L <sup>5</sup> )	-9.4

\*This value represents the mean  $\text{CO}_2$  gas exchange velocity in global oceans, estimated from the natural radiocarbon balance.

\*\*This value represents the mean  $\text{CO}_2$  gas exchange velocity in global continental shelf areas, providing a 30% reduction of the value in global oceans, as the gas exchange rate has been found to be generally less in the shelf region than in the open ocean.

<sup>1</sup>W92S: Wanninkhof's (1992) short-term formula.

<sup>2</sup>LM86: Liss and Merlivat's (1986) formula.

<sup>3</sup>T90: Tans et al.'s (1990) formula.

<sup>4</sup>W92: Wanninkhof's (1992) formula. However, the authors did not indicate that short-term or long-term formulae were used.

<sup>5</sup>W92L: Wanninkhof's (1992) long-term formula.

<sup>a</sup> Average value in the continental shelf zone west of 126.5°E.

<sup>b</sup> Average value in the continental shelf zone west of 125.5°E.

<sup>c</sup> Observations were carried out in Feb. and Oct. 1993, Aug. 1994, Nov. 1995, and Sept. 1996.

<sup>d</sup> As the original paper did not give the  $\Delta p\text{CO}_2$ , the values reported here were back-calculated from the given flux data using Wanninkhof's (1992) short-term formula. The temperature, salinity and wind speed data needed for the back calculation were taken from Tables 1 and 2 in Shim et al. (2007).

<sup>e</sup> The same as <sup>d</sup>, but using Wanninkhof's (1992) long-term formula.

<sup>f</sup> Sampling time of Zhai and Dai (2009): Spring: Apr. and May 2005, and Mar. and Apr. 2008; Summer: Aug. 2003 and July 2007; Fall: Sept., Oct. and Nov 2006, and Nov. 2007; Winter: Jan. 2006.

temperature ( $p\text{CO}_2^{\text{(seawater)}}$ ) using the empirical temperature dependence of Takahashi et al. (1993):

$$p\text{CO}_2^{\text{(seawater)}} = p\text{CO}_2^{\text{(eq)}} \times \exp\left[0.0423 \times (SST - T^{\text{(eq)}})\right],$$

where SST is the in situ sea surface temperature, and  $T^{\text{(eq)}}$  is the temperature in the equilibrator. The temperature difference between SST and  $T^{\text{(eq)}}$  ranged from approximately 0.2 to 0.5 °C.

An internal consistency check of the carbonate system was performed by comparing the measured  $p\text{CO}_2$  with the calculated  $p\text{CO}_2$ . The CO2SYS program of Lewis and Wallace (1998) was used to calculate  $p\text{CO}_2$  from three different combinations of the carbonate parameters (i.e. DIC–TA, DIC–pH, and TA–pH). Four different parameterizations for carbonic acid dissociation constants ( $K_1$  and  $K_2$ ) after Hansson (1973a,b), Mehrbach et al. (1973), Goyet and Poisson (1989), and Roy et al. (1993) were applied in the  $p\text{CO}_2$  computation in this study. The underway  $p\text{CO}_2$  measurements conducted during the occupation of the station were averaged to represent the measured  $p\text{CO}_2$  at each station. As shown in Fig. 2, the differences between measured and calculated  $p\text{CO}_2$  ranged from  $5 \pm 5$  to  $16 \pm 12 \mu\text{atm}$ .

### 2.3. Calculation of the sea-to-air $\text{CO}_2$ exchange flux

The net sea-to-air  $\text{CO}_2$  exchange flux was calculated using the formula:

$$F = ks(\Delta p\text{CO}_2),$$

where  $k$  is the  $\text{CO}_2$  gas transfer velocity,  $s$  is the solubility of  $\text{CO}_2$  (Weiss, 1974), and  $\Delta p\text{CO}_2$  is the difference between the  $p\text{CO}_2$  of water ( $p\text{CO}_2^{\text{(seawater)}}$ ) and air ( $p\text{CO}_2^{\text{(air)}}$ ). The  $p\text{CO}_2^{\text{(air)}}$  was corrected to 100% humidity using the temperature and salinity data at the time of sampling. As the underway system runs on an hourly cycle (four standards, seven headspace samples from the equilibrator and three air samples were analyzed during one cycle), the hourly averaged  $p\text{CO}_2^{\text{(air)}}$  was used to calculate the  $\Delta p\text{CO}_2$  values. The gas transfer velocity was parameterized using the Wanninkhof (1992) empirical function of long-term wind speed:

$$k = 0.39 \times u^2 \times (Sc/660)^{-0.5},$$

where  $u$  is the wind speed at 10 m height (we used monthly averaged wind speeds in January 2008 from QuikSCAT satellite data with a

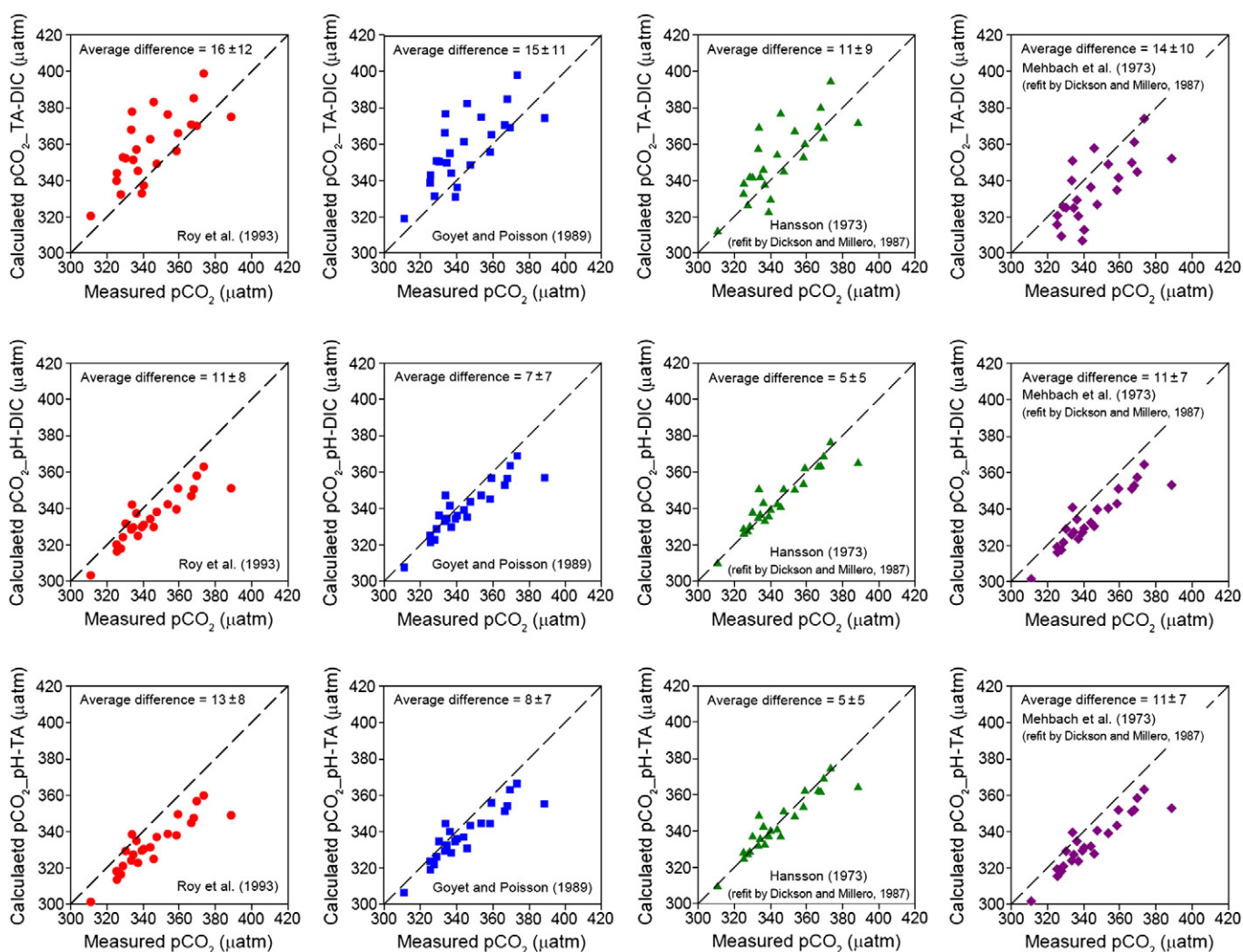


**Fig. 2.** Plots of calculated  $p\text{CO}_2$  from TA and DIC (upper panel), pH and DIC (middle panel), and pH and TA (lower panel) using four sets of dissociation constants of  $K_1$  and  $K_2$  (Roy et al., 1993; Goyet and Poisson, 1989; Hansson, 1973a,b as refitted by Dickson and Millero, 1987; Mehrbach et al., 1973 as refitted by Dickson and Millero, 1987) vs. the measured underway  $p\text{CO}_2$ . Dashed-lines are the 1:1 lines.

spatial resolution of  $0.2^\circ \times 0.2^\circ$  grids; [http://www.remss.com/qscat/qscat\\_browse.html](http://www.remss.com/qscat/qscat_browse.html)), and  $S_c$  is the Schmidt number for  $\text{CO}_2$  in seawater computed from in situ temperature data.

### 3. Results and discussion

#### 3.1. Spatial distributions of SST, SSS, and carbon parameters, and associations with the circulation pattern

The distributions of SST, SSS, and the carbon parameters (DIC,  $\text{pH}@25^\circ\text{C}$ , TA and  $p\text{CO}_2$ ) are shown in Fig. 3a–f. The SST varied from  $12.2^\circ\text{C}$ – $24.4^\circ\text{C}$  and generally paralleled the bottom topography, with a pattern toward an increase in a southeasterly direction from the mouth of the Changjiang River to the Ryukyu Island chain (Fig. 3a). The strong negative correlation between SST and depth ( $r^2 = 0.93$ ; data not shown) suggested that seafloor depth exerted strong control over SST distribution in the ECS shelf in winter (Xie et al., 2002). SSS varied from 30.64–34.62; waters of lower-SSS were confined to a narrow band along the coast of mainland China, whereas waters of highest-SSS were found in the southeastern part of the study area. Furthermore, a high salinity tongue orientated northwesterly could be traced as far as  $\sim 30.5^\circ\text{N}$ .

In general, the surface distributions of SST and SSS corresponded well to the winter circulation pattern in the ECS (Su, 2001). Waters with the highest SST and SSS, in the southeastern part of the study

area, fingerprinted the Kuroshio Current (KC in Fig. 1b), which is the western boundary current of the North Pacific Ocean flowing northeastward between 200 and 1000 m isobath along the ECS continental slope. The narrow band of waters with the lowest SST and SSS values, along the coast of mainland China, was indicative of the China Coastal Current (CCC in Fig. 1b), which is intensified by the northeastward winter monsoon and which flows southward along the coast of China in winter. The tongue of moderately high SST and SSS near  $30.5^\circ\text{N}$  represented the enhanced on-shelf intrusion of the Kuroshio Branch Current (KBC in Fig. 1b), which separates from the main stream off northeast of Taiwan and flows northeastward along the  $\sim 100$  m isobath (Liu et al., 1992).

DIC and  $\text{pH}@25^\circ\text{C}$  varied from 1941 to 2081  $\mu\text{mol kg}^{-1}$  and from 7.905 to 8.091, respectively. These distributions generally followed the seafloor bathymetry and corresponded fairly well to the overall circulation system (Fig. 3c and d). The higher DIC and lower  $\text{pH}@25^\circ\text{C}$  values occurred mainly in the inner shelf (water depth  $< 50$  m) along the coast of mainland China, associated with cold and less saline CCC water. The lower DIC and higher  $\text{pH}@25^\circ\text{C}$  values were observed in the outer shelf (water depth  $> 100$  m), in warm and saline KC water. Intermediate values of DIC and  $\text{pH}@25^\circ\text{C}$  were commonly found in the middle shelf (50 m  $<$  water depth  $< 100$  m) because of the intrusion of the KBC water. In contrast to DIC, TA values varied within a relatively narrow range, from 2240–2286  $\mu\text{mol kg}^{-1}$ , and TA distribution did

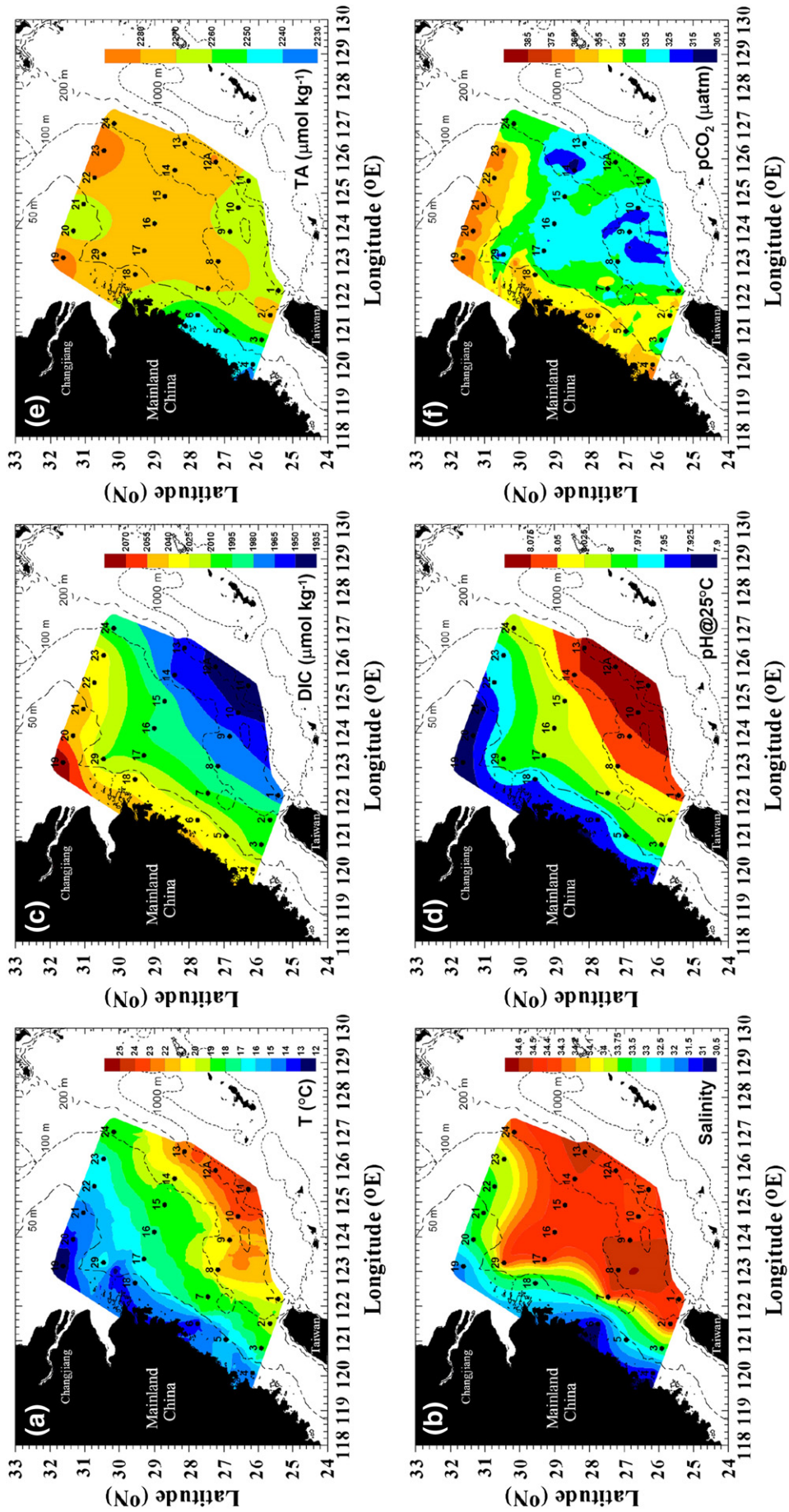


Fig. 3. Surface distributions of (a) temperature, (b) salinity, (c) DIC, (d) pH@25 °C, (e) TA and (f) pCO<sub>2</sub> in the East China Sea during winter.

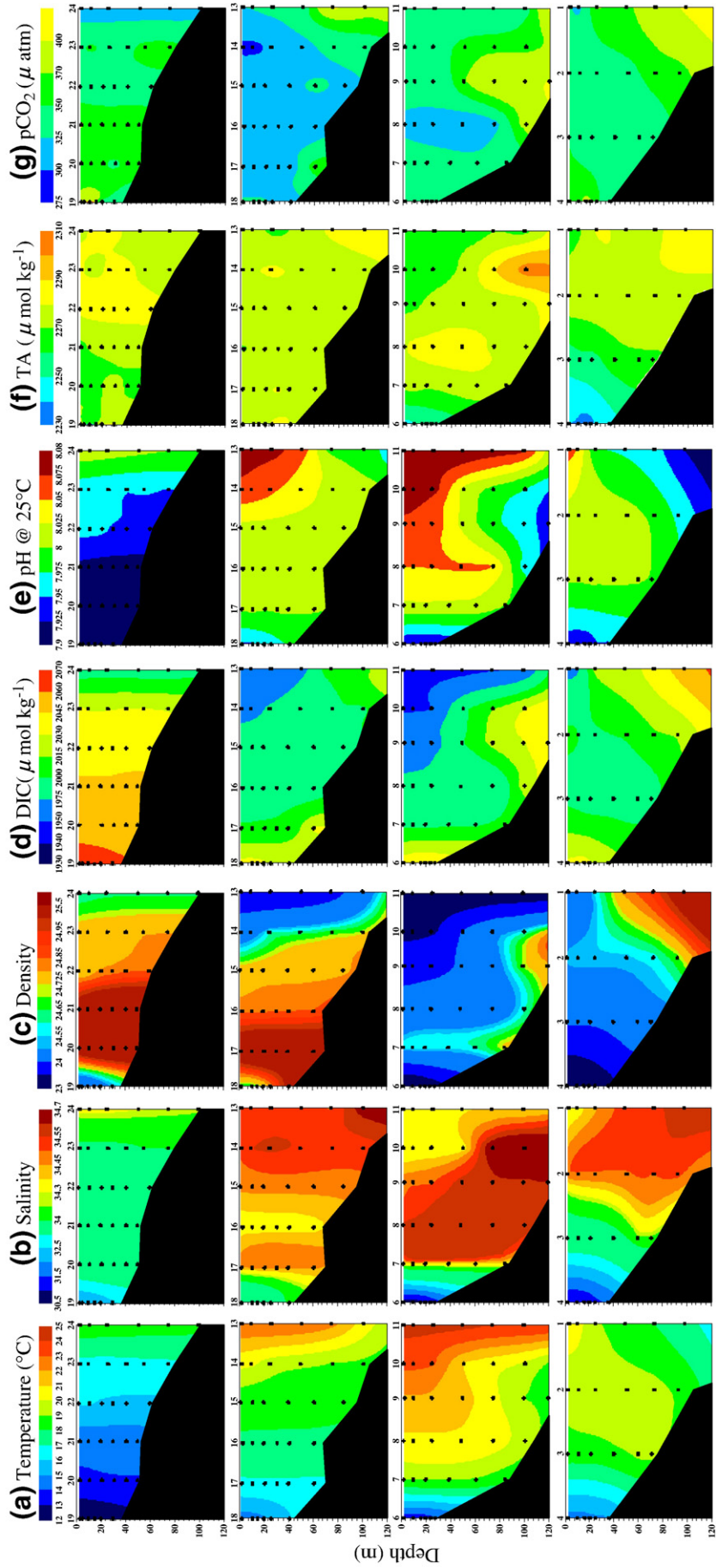


Fig. 4. Cross sections of (a) temperature, (b) salinity, (c) density, (d) DIC, (e) pH@25 °C, (f) TA and (g) pCO<sub>2</sub> along four transects investigated in this study.

not follow the seafloor bathymetry nor circulation pattern. Higher and lower TA values were generally found in the northern and southern parts of the study area, respectively (Fig. 3e). The distribution pattern of  $p\text{CO}_2$ , which ranged from 306 to 390  $\mu\text{atm}$ , was generally similar to that of DIC. Thus, higher  $p\text{CO}_2$  values were found in the inner shelf, in CCC water, whereas lower  $p\text{CO}_2$  values were generally restricted to the outer shelf, where the KC water was dominant. Intermediate  $p\text{CO}_2$  values were confined to the middle shelf, where mixing with KBC water occurred (Fig. 3f).

The vertical distributions of temperature, salinity, density and carbon parameters along the four cross shelf transects are shown in Fig. 4a–g. The vertical structure of the water column formed two distinct patterns, approximately bounded by the 100 m isobath. For stations located in the inner and middle shelves (water depth < 100 m; stations 3–7, 15–23 and 29), the vertical distributions of temperature, salinity and density were all homogenous, indicating enhanced vertical mixing in the water column, caused by intensified winter cooling and monsoonal winds. The depth profiles of carbon parameters also showed a homogenous vertical structure, suggesting that physical mixing overwhelmed biological processes in control of the vertical distribution of carbon parameters in the shallow water area

of the ECS shelf in winter. In contrast, at stations located in the outer shelf (water depth > 100 m; stations 1, 2, 8–11, 12A, 13, 14 and 24), the water column was stratified, as evidenced by increase in density with depth. The depth profiles of carbon parameters (DIC, TA and  $p\text{CO}_2$ ) in this area also increased with depth and  $\text{pH}@25^\circ\text{C}$  decreased, implying that vertical mixing is not the dominant factor in regulating the vertical distribution of carbon parameters in the outer shelf.

### 3.2. Relationships between carbon chemistry parameters and temperature, and salinity, in surface waters

The relationships between carbon chemistry parameters (*i.e.*, DIC,  $\text{pH}@25^\circ\text{C}$ , TA and  $p\text{CO}_2$ ) and the temperature of surface waters are shown in Fig. 5a–d. The strongly negative correlation between DIC and temperature ( $r^2 = 0.92$ ; open symbols and dashed line in Fig. 5a) suggests that temperature is important in controlling the spatial variation of DIC. Assuming that a water parcel with a constant TA of 2269  $\mu\text{mol kg}^{-1}$  (the average of surface TA measurements) is in equilibrium with an atmospheric  $p\text{CO}_2$  of 388  $\mu\text{atm}$  (the average of the atmospheric  $p\text{CO}_2$  measurements), the temperature dependence of DIC variation in this hypothetical water parcel can be calculated

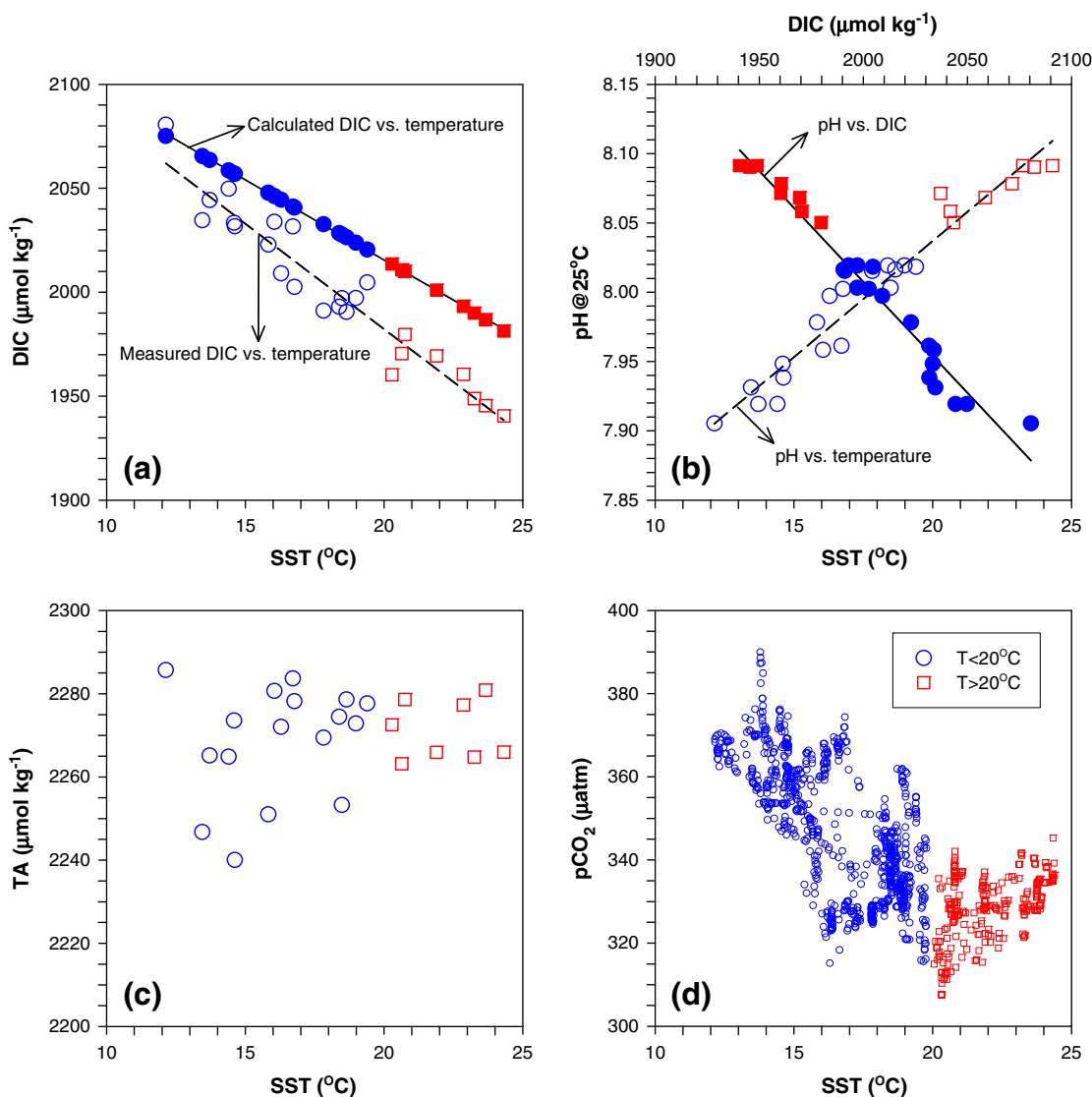


Fig. 5. Plots of (a) measured and calculated DIC, (b)  $\text{pH}@25^\circ\text{C}$ , (c) TA and (d)  $p\text{CO}_2$  vs. temperature for surface waters in the East China Sea during winter. The plot of  $\text{pH}@25^\circ\text{C}$  vs. DIC is superimposed on (b). Square and circle symbols represent water samples with temperature higher and lower than  $20^\circ\text{C}$ , respectively.

as  $-7.7 \mu\text{mol kg}^{-1} \text{ } ^\circ\text{C}^{-1}$  (solid symbols and line in Fig. 5a). This value is less than the observed slope of the DIC–temperature relationship (slope =  $-10.1 \mu\text{mol kg}^{-1} \text{ } ^\circ\text{C}^{-1}$ ), implying that factor(s) other than temperature may influence DIC variation. Fig. 5a further shows that the difference between the theoretically equilibrated (solid symbols) and observed (open symbols) DIC values declined with decreasing temperature, implying that additional DIC source(s) in these low-temperature waters may have been derived from respired  $\text{CO}_2$  that accumulated in bottom waters in summer, when the water column was strongly stratified.

As shown in Fig. 6, DIC levels in bottom waters at the shallow water stations were much higher than those at deeper water stations during summer, whereas the saturation level of dissolved oxygen showed the opposite trend (data from Chou et al., 2009b). This dichotomy can best be explained by the increased accumulation of remineralized  $\text{CO}_2$  in bottom waters at the shallower stations, where the supply of particulate organic carbon from the overlying surface layer is elevated because of high nutrient inputs from the Changjiang River (Gong et al., 1996; Gong et al., 2003). However, shoaling of the seafloor in the inner shelf might also play a role in the accumulation of more respired  $\text{CO}_2$  in the water column as such  $\text{CO}_2$  storage in shallower areas would be enhanced by constant benthic flux (i.e.,  $\text{CO}_2$  efflux from sediment to the water column). Enhanced accumulation of remineralized  $\text{CO}_2$  in bottom waters during the period of stratification would therefore provide more DIC to surface waters when stratification collapsed, thus reducing the difference between the calculated and observed DIC in the inner shelf, an area characterized by low-temperature seawater. Zhai and Dai (2009) recently reported that the inner shelf near the Changjiang River estuary acts as a significant sink of atmospheric  $\text{CO}_2$  during winter, spring and summer seasons, but a net source of  $\text{CO}_2$  in autumn. This autumn reversal, during transition from summer to winter, could result from vertical mixing of  $\text{CO}_2$ -rich subsurface waters, consistent with the process proposed earlier. In summary, our results indicate that, in addition to temperature, the extent of  $\text{CO}_2$  enhancement in bottom waters before the collapse of stratification may play an important role in controlling DIC variation in the ECS in winter, especially in the inner and middle shelves, where the entire water column is well mixed.

Although there was a strong correlation between  $\text{pH@25 } ^\circ\text{C}$  and temperature ( $r^2 = 0.94$ ; open symbols and dashed line in Fig. 5b), the observed  $\text{pH@25 } ^\circ\text{C}$  variation cannot be directly ascribed to a temperature effect because the  $\text{pH@25 } ^\circ\text{C}$  values reported in this study were all obtained at  $25 } ^\circ\text{C}$ . As noted in Section 3.1, the variation in surface DIC was much greater than that of TA ( $140$  vs.  $38 \mu\text{mol kg}^{-1}$ ), implying that DIC concentration may play a major role in regulating

$\text{pH@25 } ^\circ\text{C}$  variation. A strong negative correlation between  $\text{pH@25 } ^\circ\text{C}$  and DIC ( $r^2 = 0.96$ ; solid symbols and line) is also evident in Fig. 5b, suggesting that the underlying processes controlling the spatial variation of  $\text{pH@25 } ^\circ\text{C}$  are similar to those affecting variation in DIC. Unlike DIC and  $\text{pH@25 } ^\circ\text{C}$ , TA was not strongly correlated with SST (Fig. 5c). This is because the effect of temperature on the solubility of  $\text{CO}_2$  and the dissociation constant of carbonic acid can lead to changes in DIC and  $\text{pH@25 } ^\circ\text{C}$ , but  $\text{CO}_2$  flux to or from the atmosphere does not change the TA.

The correlations between underway  $\text{pCO}_2$  measurements and SST showed two opposing trends (Fig. 5d): a positive correlation for waters with  $\text{SST} > 20 } ^\circ\text{C}$  (open squares), and a negative correlation for waters with  $\text{SST} < 20 } ^\circ\text{C}$  (open circles). The positive correlation for waters with  $\text{SST} > 20 } ^\circ\text{C}$  indicates that temperature is the major factor controlling spatial variations in  $\text{pCO}_2$  level in the outer shelf, where it is covered by the KC and the water column remains stratified (note that the  $20 } ^\circ\text{C}$  isotherm corresponds well to  $100$  m isobath; Fig. 3a). A positive correlation between  $\text{pCO}_2$  and SST was also found in other seasons in the KC-affected area of the ECS (Rehder and Suess, 2001; Shim et al., 2007; Liu et al., 2008). Therefore, temperature seems to be the predominant factor in regulating annual  $\text{pCO}_2$  variation in the KC waters. For the waters with an  $\text{SST} < 20 } ^\circ\text{C}$  the negative correlation between  $\text{pCO}_2$  and SST suggests that other factor(s) may overwhelm temperature in controlling  $\text{pCO}_2$  in the vertically well-mixed inner and middle shelves. A similar negative relationship has recently been reported in the southern Yellow Sea in winter (Zhang et al., 2010). As noted earlier, summer accumulations of remineralized  $\text{CO}_2$  in bottom waters of the inner shelf could be readily transported to surface waters via strong vertical mixing in winter. As a result, the  $\text{pCO}_2$  of the surface waters of the inner shelf is high relative to that in the middle shelf, where less  $\text{CO}_2$  accumulates in bottom waters during the stratification period, leading to the observed negative correlation between  $\text{pCO}_2$  and SST for these low-temperature waters.

Fig. 7a–d shows the relationships between carbon chemistry parameters and salinity for surface waters. The superimposed dashed lines in Fig. 7 represent the hypothetical mixing lines between the fresh and seawater end-members. The carbon chemistry data reported by Zhai et al. (2007) for the Changjiang River in winter were used as fresh water end-member, whereas the averaged surface data at stations 10, 11 and 12A of the present study were chosen to represent the seawater end-member. It is noteworthy that the mixing lines of DIC,  $\text{pH@25 } ^\circ\text{C}$  and TA vs. salinity are all linear, whereas that of  $\text{pCO}_2$  vs. salinity is non-linear. The latter relationship was derived from conservative mixing of TA, DIC and temperature data using freshwater and seawater values as the two end-members. The plots of DIC,  $\text{pH@25 } ^\circ\text{C}$  and  $\text{pCO}_2$  vs. salinity (Fig. 7a, b and d, respectively) show that these parameters do not follow the hypothetical mixing lines. This implies that vertical mixing is more important than is horizontal mixing in regulating the distributions of DIC,  $\text{pH@25 } ^\circ\text{C}$  and  $\text{pCO}_2$ , because strong mixing in winter would bring subsurface/bottom water (high DIC and  $\text{pCO}_2$  but low  $\text{pH@25 } ^\circ\text{C}$ ) upwards into the surface layer. In contrast, the comparatively fair agreement between the TA–salinity correlation and the hypothetical mixing line (Fig. 7c) can be attributed to the small change in TA gradient with depth during the stratification period (Chou et al., 2009a,b).

### 3.3. $\Delta\text{pCO}_2$ and sea–air $\text{CO}_2$ exchange flux

The  $\Delta\text{pCO}_2$  ( $\text{pCO}_2^{\text{water}} - \text{pCO}_2^{\text{air}}$ ) and the sea–air  $\text{CO}_2$  exchange flux are shown along the cruise tracks in Fig. 8. The  $\Delta\text{pCO}_2$  values ranged from  $-0$  to  $-111 \mu\text{atm}$ , with an average value of  $-46 \mu\text{atm}$ . The negative  $\Delta\text{pCO}_2$  values indicate that the entire ECS shelf acted as a sink for atmospheric  $\text{CO}_2$  in winter. Furthermore, as atmospheric  $\text{pCO}_2$  remained within a relatively narrow range ( $388 \pm 12 \mu\text{atm}$ ); the standard deviation on the mean of atmospheric  $\text{pCO}_2$  suggests a landmass influence (Borges and Frankignoulle, 2001, and references

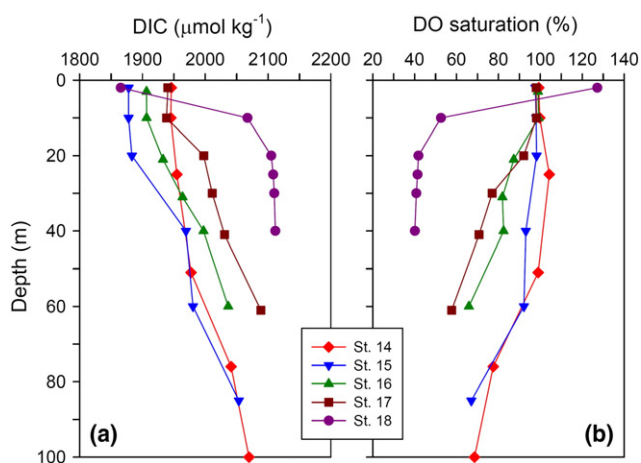


Fig. 6. Depth distributions of (a) DIC and (b) dissolved oxygen saturation at stations 14–18 in July 2007. Data from Chou et al. (2009b).

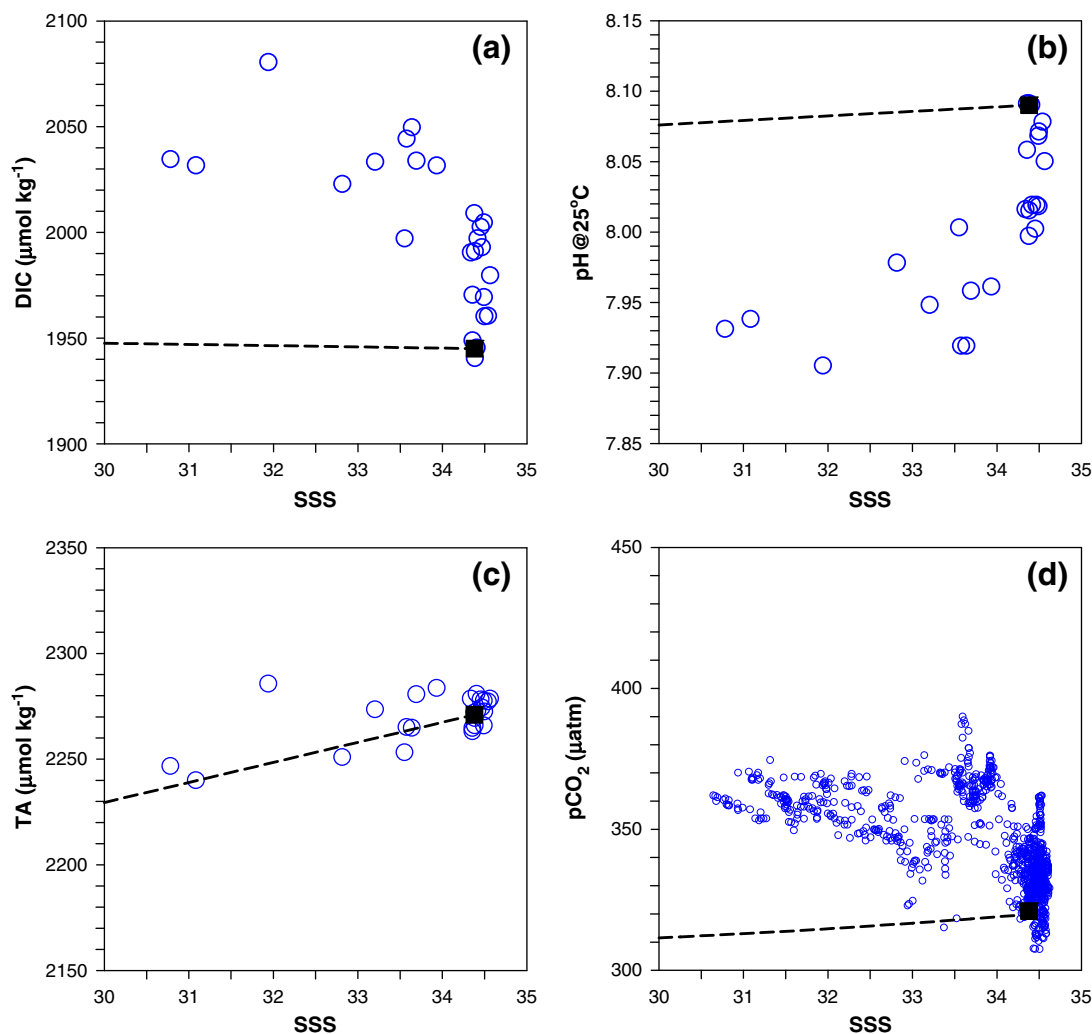


Fig. 7. Plots of (a) DIC, (b) pH@25 °C, (c) TA and (d) pCO<sub>2</sub> vs. salinity for the surface waters in the East China Sea during winter. The superimposed dashed lines represent the hypothetical conservative mixing lines between the fresh water and seawater end-members.

therein), the  $\Delta p\text{CO}_2$  variation was controlled primarily by the pCO<sub>2</sub> of surface seawater. As a result, the distribution of  $\Delta p\text{CO}_2$  generally paralleled that of surface pCO<sub>2</sub> (Fig. 3f), with lower values in the inner and northern middle shelf, and higher values in the outer and central middle shelf. Also, as shown in Fig. 8b the sea-air CO<sub>2</sub> exchange flux ranged from  $\sim 0$  to  $\sim -30$  mmol C m<sup>-2</sup> day<sup>-1</sup>, with an average value of  $-13.7 \pm 5.3$  mmol C m<sup>-2</sup> day<sup>-1</sup>. As the monthly satellite wind speed data used to calculate the CO<sub>2</sub> gas transfer velocity (*k*) did not show any marked spatial variation in the study area ( $9.7 \pm 1.0$  m s<sup>-1</sup>), the flux variability was dominated mainly by  $\Delta p\text{CO}_2$ . Accordingly, the distribution pattern of sea-air CO<sub>2</sub> exchange flux mimicked that of  $\Delta p\text{CO}_2$ .

Table 1 summarizes the sea-air CO<sub>2</sub> exchange fluxes derived from this study and from previous reports on the ECS. As diverse sources of wind speed data and parameterizations of gas transfer velocity were used in previous studies (see Table 1 for a summary), we applied a uniform source of monthly wind speed data from NCEP (<http://www.esrl.noaa.gov/psd/data/gridded/reanalysis/>) and the gas transfer algorithm of Wanninkhof (1992; long-term formula) to re-calculate earlier values. The results show that the flux estimated in the present study is the highest reported for the ECS, either in winter or annually. The value obtained ( $-9.4$  mmol C m<sup>-2</sup> day<sup>-1</sup>) is greater than both those re-calculated from Tsunogai et al. (1997;  $-6.2$  mmol C m<sup>-2</sup> day<sup>-1</sup>) along the PN line and from Zhai and Dai (2009;  $-5.9$  mmol C m<sup>-2</sup> day<sup>-1</sup>) in the inner shelf near the Changjiang River estuary. Considering the

seasonal average of re-calculated fluxes summarized in Table 1, winter ( $-7.2 \pm 1.9$  mmol C m<sup>-2</sup> day<sup>-1</sup>) appears to be the most important season for influx of atmospheric CO<sub>2</sub> into the ECS, with such flux being  $\sim 5.5$ -fold greater than in spring ( $-1.3 \pm 0.9$  mmol C m<sup>-2</sup> day<sup>-1</sup>),  $\sim 5.2$ -fold greater than in summer ( $-1.4 \pm 1.7$  mmol C m<sup>-2</sup> day<sup>-1</sup>),  $\sim 8.0$ -fold greater than in autumn ( $-0.9 \pm 4.8$  mmol C m<sup>-2</sup> day<sup>-1</sup>). The annual mean flux (the average of the seasonal recomputed fluxes) was estimated to be  $-2.7$  mmol C m<sup>-2</sup> day<sup>-1</sup>, thus approximately 34% of the estimate ( $-8.0$  mmol C m<sup>-2</sup> day<sup>-1</sup>) reported by Tsunogai et al. (1999), suggesting that their result may be an overestimate.

#### 3.4. Comparison with previous studies: implications for changes of pCO<sub>2</sub> vs. SST relationship and $\Delta p\text{CO}_2$

Fig. 9 shows a comparison of the atmospheric and surface water pCO<sub>2</sub> and SST values along the PN line, reported by Tsunogai et al. (1997, 1999; data collected in February 1993), with those determined along the most northern transect in the present study (data collected in January 2008). The atmospheric pCO<sub>2</sub> increased from 360 μatm (the horizontal dotted lines in Fig. 9a), and the change corresponds well with variation observed at Cheju Island (33.28°N, 126.15°E; an increase from 360 μatm in February 1993 to 387 μatm in January 2008; [http://www.esrl.noaa.gov/gmd/ccgg/globalview/co2/co2\\_intro.html](http://www.esrl.noaa.gov/gmd/ccgg/globalview/co2/co2_intro.html)). However, unlike what was seen by Tsunogai et al. (1997, 1999; solid squares and line in Fig. 9a), pCO<sub>2</sub> along the most

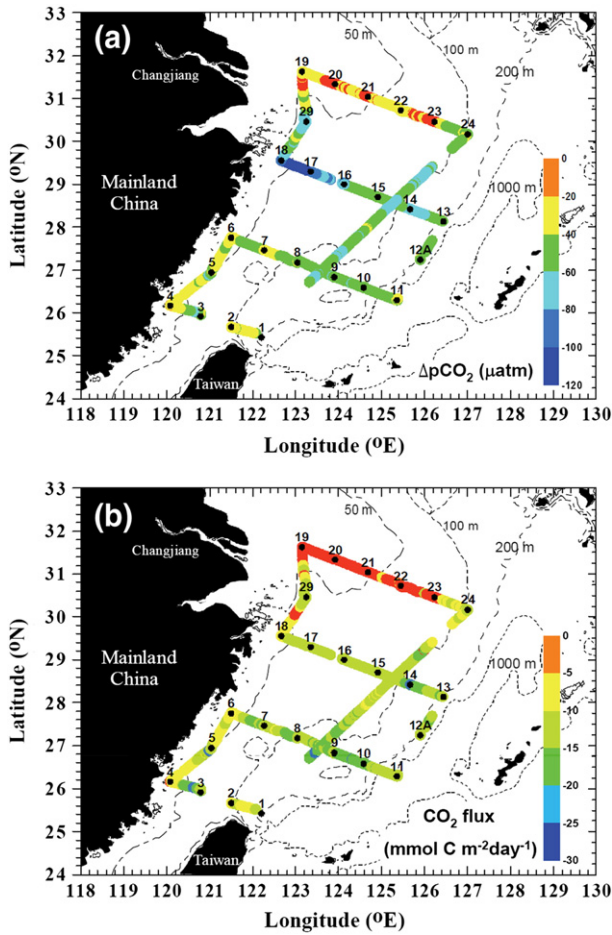


Fig. 8. Surface distributions of (a) sea-to-air pCO<sub>2</sub> difference ( $\Delta pCO_2$ ) and (b) sea-to-air CO<sub>2</sub> exchange flux in the East China Sea during winter.

northern transect of the present study (open circles and solid line in Fig. 9a) did not show an increasing offshore trend, even though both studies found similarly increasing SST trends (Fig. 9b). Likewise, Tsunogai et al. (1997, 1999) reported a strong positive correlation ( $r^2=0.94$ , solid circles and line in Fig. 10) between pCO<sub>2</sub> and SST along the PN line, but, in the present study, a negative correlation ( $r^2=0.40$ , open squares and dashed line in Fig. 10) was observed when data from the two most northern transects were analyzed. As noted in Section 3.2, the negative correlation between pCO<sub>2</sub> and SST seen in the present study may reflect greater accumulation of respired CO<sub>2</sub> in bottom waters of the inner shelf, compared to the middle and outer shelves, during summer, when the water column is stratified. The contrasting positive correlation reported by Tsunogai et al. (1997, 1999) thus suggests that the enhanced summer accumulation of respired CO<sub>2</sub> in the inner shelf did not occur in 1993, and that summer accumulation of CO<sub>2</sub> in bottom waters may have substantially increased between 1993 and 2008.

Assuming that the rate of pCO<sub>2</sub> increase in surface waters between February 1993 and January 2008 is the same as that for the atmospheric pCO<sub>2</sub> ( $1.87 \mu atm yr^{-1}$ ), the increase of atmospheric pCO<sub>2</sub> was added to the surface water pCO<sub>2</sub> along the PN line in 1993. After correction of the effect of the atmospheric pCO<sub>2</sub> increment, the effect of a temperature difference between the PN line and the most northern transect of the present study (Fig. 9b) was further corrected using a temperature effect coefficient of  $4.23\% \text{ } ^\circ C^{-1}$  (Takahashi et al., 1993). After correction of both the atmospheric pCO<sub>2</sub> increase and the temperature difference, the hypothetical pCO<sub>2</sub> along the PN line in 2008 (the dashed line with open squares in Fig. 9a) is generally in good agreement with measured pCO<sub>2</sub> values along the most northern

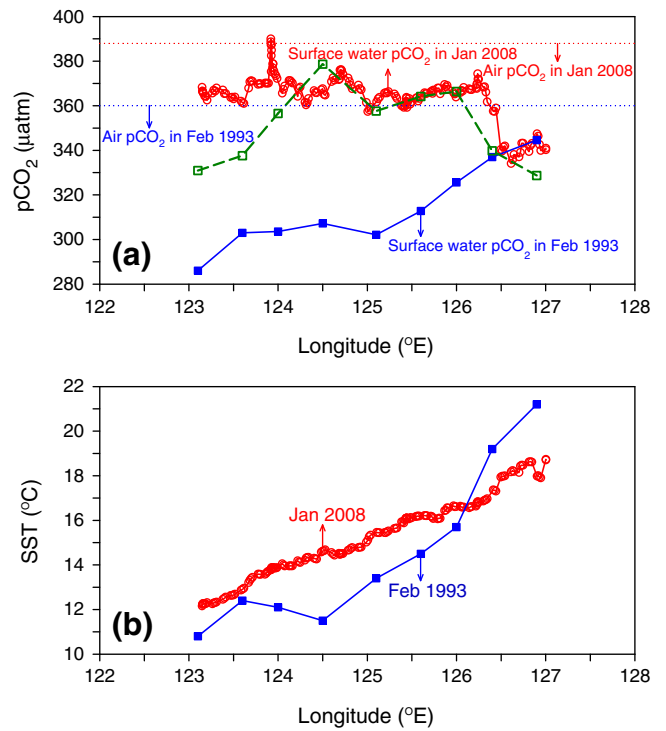


Fig. 9. Distributions of (a) atmospheric pCO<sub>2</sub> and pCO<sub>2</sub> in surface water, and (b) SST along the PN line in February 1993 and along the most northern transect in this study (January 2008). Data for 1993 are derived from Tsunogai et al. (1999). The superimposed dashed line with open squares in panel (a) represents the hypothetical surface water pCO<sub>2</sub> along the PN line in 2008, derived from the surface water pCO<sub>2</sub> of 1993 after correcting for the increase in atmospheric pCO<sub>2</sub> and temperature differences between 1993 and 2008.

transect of January 2008, for the area east of 124.5°E. In contrast, the hypothetical pCO<sub>2</sub> value is substantially lower than the measured pCO<sub>2</sub> figures in the area west of 124.5°E. This discrepancy can also be attributed to an increase in the summer accumulation of respired CO<sub>2</sub> in the inner shelf near the Changjiang River estuary between 1993 and 2008, since the subsequent breakdown of stratification would supply more CO<sub>2</sub> from bottom water.

Tsunogai et al. (1997) reported an average  $\Delta pCO_2$  of  $-63 \mu atm$  in February 1993 for the inner shelf zone along the PN line (west of

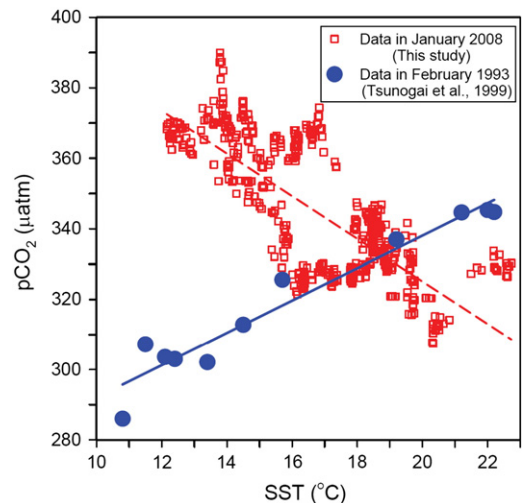


Fig. 10. Plot of surface water pCO<sub>2</sub> vs. SST for the data collected in January 2008 in this study along the two most northern transects (open squares), and for the data collected along the PN line in February 1993 (Tsunogai et al., 1999; solid circles).

125.5°E). However, Zhai and Dai (2009) documented a mean  $\Delta p\text{CO}_2$  of  $-37 \pm 17 \mu\text{atm}$  in January 2006 for the inner shelf of the ECS off the Changjiang River estuary. Our study explored a similar area (30–31.5°N and 123–125.5°E), and we found a slightly lower average  $\Delta p\text{CO}_2$  ( $-30 \pm 18 \mu\text{atm}$ ;  $n = 197$ ) in January 2008. These results suggest that the wintertime  $\Delta p\text{CO}_2$  in the inner shelf near the Changjiang River estuary may have appreciably decreased between the 1990s and the 2000s. As the  $p\text{CO}_2$  level in the Changjiang River has fallen in the last 30 years (Wang et al., 2007), the observed reduction of  $\Delta p\text{CO}_2$  in the inner shelf near the Changjiang River estuary cannot be attributed to a change in riverine  $p\text{CO}_2$  level. Likewise, Tsunogai et al. (1997) reported that the inner shelf near the PN line acted as a strong sink for atmospheric  $\text{CO}_2$  in autumn (October) 1993 ( $\Delta p\text{CO}_2 = -44 \mu\text{atm}$ ; Table 1). However, Zhai and Dai (2009) found that, in a similar area during autumn (November) 2006 and 2007, the shelf acted as a  $\text{CO}_2$  source (average  $\Delta p\text{CO}_2 = 11 \mu\text{atm}$ ; Table 1). Shim et al. (2007) reported that the western part of the northern ECS (31.5–34.0°N and 124.0–126.5°E) acted as a  $\text{CO}_2$  source in autumn 2004 and 2005 (October and November, respectively; average  $\Delta p\text{CO}_2 = 7 \mu\text{atm}$ ; Table 1). These results indicate that  $\Delta p\text{CO}_2$  in autumn has changed from negative to positive values over recent decades. The  $\Delta p\text{CO}_2$  (absolute value) decrease in autumn and winter between the 1990s and the 2000s may also be explained by the enhanced summer accumulation of respired  $\text{CO}_2$ , as when the seasonal overturn takes place, more respired  $\text{CO}_2$  can be brought into the surface, and therefore may decrease  $\Delta p\text{CO}_2$ .

As mentioned in the “Introduction”, it is well known that eutrophication/hypoxia has significantly increased off the Changjiang River estuary over the past decades. The deteriorating eutrophication/hypoxia would lead to more respired  $\text{CO}_2$  accumulated in bottom water during the summertime, as suggested by the  $p\text{CO}_2$  vs. SST relationship which has shifted from positive to negative and  $\Delta p\text{CO}_2$  has markedly decreased between the 1990s and the 2000s. Considering the high intra-seasonal and inter-annual variations in the ECS, more long-term studies are, therefore, needed to unveil the potential impacts of eutrophication/hypoxia on the capacity of  $\text{CO}_2$  sequestration in the ECS, and in other coastal seas as well.

#### 4. Summary and concluding remarks

We have described the spatial distributions of DIC,  $\text{pH}@25^\circ\text{C}$ , TA, and  $p\text{CO}_2$ , and discussed relationships between these parameters and the general circulation pattern, temperature, and salinity in the ECS, based on data obtained from four cross shelf transects conducted in January 2008. We found that temperature was the dominant factor controlling the spatial variation of carbon parameters in the outer shelf, where the water column is well stratified. However, the degree of  $\text{CO}_2$  enrichment in bottom waters prior to the water column becoming overturned regulated DIC,  $\text{pH}@25^\circ\text{C}$ , and  $p\text{CO}_2$  levels in the inner and middle shelves, where the entire water column is vertically well mixed in winter. When the results of this study, and re-calculated fluxes (using monthly wind speeds from NCEP and the gas transfer algorithm of Wanninkhof (1992; long-term formula) from prior reports were compared, it was apparent that winter is the most important season for  $\text{CO}_2$  absorption in the ECS.

Furthermore, comparisons of data from the present and previous studies show that there was a positive correlation between  $p\text{CO}_2$  and SST in the northern ECS in winter in 1993, but a negative relationship in 2008, and that  $\Delta p\text{CO}_2$  in the inner shelf near the Changjiang River estuary in winter has noticeably declined since 1993. Though the increased eutrophication/hypoxia in the inner shelf near the Changjiang River estuary over recent decades could be one of the potential driving forces causing these observed changes, the fundamental relationship between the changes in carbonate chemistry and the increased eutrophication/hypoxia in the ECS certainly warrant further long-term studies.

#### Acknowledgements

We are grateful to the captain, crew and technicians of the *R/V Ocean Researcher I* for shipboard operation and water sampling, and to T. F. Tseng and Y. F. Chen for laboratory assistance. Constructive comments from two anonymous reviewers have greatly improved the manuscript. This work was supported by the National Science Council of the Republic of China (grant nos. NSC 98-2611-M-019-013 and NSC 98-2611-M-019-014-MY3) and the Center for Marine Bioenvironment and Biotechnology of the National Taiwan Ocean University.

#### References

- Beardsley, R.C., Limeburner, R., Yu, H., Cannon, G.A., 1985. Discharge of the Changjiang (Yangtze River) into the East China Sea. *Cont. Shelf Res.* 4, 57–76.
- Borges, A.V., Frankignoulle, M., 2001. Short-term variations of the partial pressure of  $\text{CO}_2$  in surface waters of the Galician upwelling system. *Prog. Oceanogr.* 51, 283–302.
- Borges, A.V., Gypens, N., 2010. Carbonate chemistry in the coastal zone responds more strongly to eutrophication than ocean acidification. *Limnol. Oceanogr.* 55, 346–353.
- Borges, A.V., Delille, B., Frankignoulle, M., 2005. Budgeting sinks and sources of  $\text{CO}_2$  in the coastal ocean: diversity of ecosystems counts. *Geophys. Res. Lett.* 32, L14601. doi:10.1029/2005GL023053.
- Cai, W.-J., Wang, Y.C., 1998. The chemistry, fluxes and sources of carbon dioxide in the estuarine waters of the Satilla and Altamaha Rivers, Georgia. *Limnol. Oceanogr.* 43, 657–668.
- Cai, W.-J., Dai, M., Wang, Y., 2006. Air–sea exchange of carbon dioxide in ocean margins: a province-based synthesis. *Geophys. Res. Lett.* 33, L12603. doi:10.1029/2006GL026219.
- Chen, C.T.A., Borges, A.V., 2009. Reconciling opposing views on carbon cycling in the coastal ocean: continental shelves as sinks and near-shore ecosystems as sources of atmospheric  $\text{CO}_2$ . *Deep Sea Res. II* 56, 578–590.
- Chen, C.C., Gong, G.C., Shiah, F.K., 2007. Hypoxia in the East China Sea: one of the largest coastal low-oxygen areas in the world. *Mar. Environ. Res.* 64, 399–408.
- Chou, W.C., Sheu, D.D., Chen, C.T.A., Wang, S.L., Tseng, C.M., 2005. Seasonal variability of carbon chemistry at the SEATS time-series site, northern South China Sea between 2002 and 2003. *Terr. Atmos. Ocean. Sci.* 16, 445–465.
- Chou, W.C., Chen, Y.L.L., Sheu, D.D., Shih, Y.Y., Han, C.A., Cho, C.L., Yang, Y.J., Tseng, C.M., 2006. Estimated net community production during the summer season at the SEATS site: implications for nitrogen fixation. *Geophys. Res. Lett.* 33, L22610. doi:10.1029/2005GL025365.
- Chou, W.C., Sheu, D.D., Lee, B.S., Tseng, C.M., Chen, C.T.A., Wang, S.L., Wong, G.T.F., 2007a. Depth distributions of alkalinity,  $\text{TCO}_2$ , and  $\delta^{13}\text{C}_{\text{TCO}_2}$  at SEATS time-series site in the northern South China Sea. *Deep-Sea Res. II* 54, 1469–1485.
- Chou, W.C., Sheu, D.D., Chen, C.T.A., Wen, L.S., Yang, Y., Wei, C.L., 2007b. Transport of the South China Sea subsurface water outflow and its influence on carbon chemistry of Kuroshio waters off southeastern Taiwan. *J. Geophys. Res.* 112, C12008. doi:10.1029/2007JC004087.
- Chou, W.C., Gong, G.C., Sheu, D.D., Hung, C.C., Tseng, T.F., 2009a. The surface distributions of carbon chemistry parameters in the East China Sea in summer 2007. *J. Geophys. Res.* 114, C07026. doi:10.1029/2008JC005128.
- Chou, W.C., Gong, G.C., Sheu, D.D., Jen, S., Hung, C.C., Chen, C.C., 2009b. Reconciling the paradox that the heterotrophic waters of the East China Sea shelf act as a significant  $\text{CO}_2$  sink during the summertime: evidence and implications. *Geophys. Res. Lett.* 36, L15607. doi:10.1029/2009GL038475.
- da Cunha, L.C., Buitenhuis, E.T., Le Quééré, C., Giraud, X., Ludwig, W., 2007. Potential impact of changes in river nutrient supply on global ocean biogeochemistry. *Glob. Biogeochem. Cycles* 21 (GB4007). doi:10.1029/2006GB002718.
- Dai, A.G., Trenberth, K.E., 2002. Estimates of freshwater discharge from continents: latitudinal and seasonal variations. *J. Hydrometeorol.* 3, 666–687.
- Dickson, A.G., Millero, F.J., 1987. A comparison of the equilibrium constants for the dissociation constants of carbonic acid in seawater media. *Deep-Sea Res.* 34, 1733–1743.
- Dickson, A.G., Sabine, C.L., Christian, J.R. (Eds.), 2007. Guide to best practices for ocean  $\text{CO}_2$  measurements: PICES special publication, 3. 191pp.
- Feely, R.A., Wanninkhof, R., Milburn, H.B., Cosca, C.E., Stapp, M., Murphy, P.P., 1998. A new automated underway system for making high precision  $p\text{CO}_2$  measurements onboard research ships. *Anal. Chim. Acta* 377, 185–191.
- Gong, G.-C., Lee Chen, Y.-L., Liu, K.-K., 1996. Chemical hydrography and chlorophyll a distribution in the East China Sea in summer: implications in nutrient dynamics. *Cont. Shelf Res.* 16, 1561–1590.
- Gong, G.-C., Wen, Y.-H., Wang, B.-W., Lin, G.-J., 2003. Seasonal variation of chlorophyll a concentration, primary production and environmental conditions in the subtropical East China Sea. *Deep Sea Res. II* 50, 1219–1236.
- Gong, G.-C., Chang, J., Chiang, K.-P., Hsiung, T.-M., Hung, C.-C., Duan, S.-W., Codispoti, L.A., 2006. Reduction of primary production and changing of nutrient ratio in the East China Sea: effect of the Three Gorges Dam? *Geophys. Res. Lett.* 33, L07610. doi:10.1029/2006GL025800.
- Goyet, C., Poisson, A., 1989. New determination of carbonic acid dissociation constants in seawater as a function of temperature and salinity. *Deep-Sea Res.* 36, 1635–1654.
- Gypens, N., Borges, A.V., Lancelot, C., 2009. Effect of eutrophication on air–sea  $\text{CO}_2$  fluxes in the coastal Southern North Sea: a model study of the past 50 years. *Glob. Change Biol.* 15, 1040–1056.

- Hansson, I., 1973a. A new set of acidity constants for carbonic acid and boric acid in sea water. *Deep-Sea Res.* 20, 461–478.
- Hansson, I., 1973b. The determination of dissociation constants of carbonic acid in synthetic seawater in the salinity range of 20–40‰ and the temperature range of 5–30 °C. *Acta Chim. Scand.* 27, 931–944.
- Johnson, K.M., Wills, K.D., Butler, D.B., Johnson, W.K., Wong, C.S., 1993. Coulometric total carbon dioxide analysis for marine studies: maximizing the performance of an automated continuous gas extraction system and coulometric detector. *Mar. Chem.* 44, 167–189.
- Lewis, E., Wallace, D.W.R., 1998. Program developed for CO<sub>2</sub> System Calculations, Carbon Dioxide Information Analysis Center, Report ORNL/CDIAC-105, Oak Ridge National Laboratory, Oak Ridge, TN, USA.
- Li, M., Xu, K., Watanabe, M., Chen, Z., 2007. Long-term variations in dissolved silicate, nitrogen, and phosphorus flux from the Yangtze River into the East China Sea and impacts on estuarine ecosystem. *Mar. Environ. Res.* 64, 399–408.
- Liss, P.S., Merlivat, L., 1986. Air–sea gas exchange rates: introduction and synthesis. In: Buatmenard, P. (Ed.), *The Role of Air–Sea Exchange in Geochemical Cycling*. Reidel, Dordrecht, Netherlands, pp. 113–127.
- Liu, K.K., Gong, G.C., Shyu, C.Z., Pai, S.C., Wei, C.L., Chao, S.Y., 1992. Response of Kuroshio upwelling to the onset of the Northeast Monsoon in the Sea North of Taiwan: observations and a numerical simulation. *J. Geophys. Res.* 97, 12511–12526.
- Liu, C., Zhang, C., Yang, X., Gong, H., Zhang, Z., 2008. A multilayer study of pCO<sub>2</sub> in the surface waters of the Yellow and South China Seas in spring and the sea–air carbon dioxide flux. *J. Ocean Univ. Chin.* 7, 263–268.
- Mackenzie, F.T., Lerman, A., Andersson, A.J., 2004. Past and present of sediment and carbon biogeochemical cycling models. *Biogeosciences* 1, 11–32.
- Mehrbach, C., Culbertson, C.H., Hawley, J.E., Pytkowicz, R.M., 1973. Measurement of the apparent dissociation constants of carbonic acid in seawater at atmospheric pressure. *Limnol. Oceanogr.* 18, 897–907.
- Peng, T.-H., Hung, J.-J., Wanninkhof, R., Millero, F.J., 1999. Carbon budget in the East China Sea. *Tellus* 51B, 531–540.
- Rabouille, C., Conley, D.J., Dai, M.H., Cai, W.-J., Chen, C.T.A., Lansard, B., Green, R., Yin, K., Harrison, P.J., Dagg, M., McKee, B., 2008. Comparison of hypoxia among four river-dominated ocean margins: the Changjiang (Yangtze), Mississippi, Pearl, and Rhône rivers. *Cont. Shelf Res.* 28, 1527–1537.
- Rehder, G., Suess, E., 2001. Methane and pCO<sub>2</sub> in the Kuroshio and the South China Sea during maximum summer surface temperature. *Mar. Chem.* 75, 89–108.
- Roy, R.N., Roy, L.N., Vogel, K.M., Pearson, T., Porter-Moore, Good, C.E., Millero, F.J., Campbell, D.M., 1993. The dissociation constants of carbonic acid in seawater at salinities 5 to 45 and temperatures 0 to 45 °C. *Mar. Chem.* 44, 249–267.
- Sheu, D.D., Chou, W.C., Chen, C.T.A., Wei, C.L., Hsieh, H.L., Hou, W.P., Dai, M.H., 2009. Riding over the Kuroshio current from the South to the East China Sea: mixing and transport of DIC. *Geophys. Res. Lett.* 36, L07603. doi:10.1029/2008GL037017.
- Shim, J., Kim, D., Kang, Y.C., Lee, J.H., Jang, S.T., Kim, C.H., 2007. Seasonal variations in pCO<sub>2</sub> and its controlling factors in surface seawater of the northern East China Sea. *Cont. Shelf Res.* 27, 2623–2636.
- Su, J.L., 2001. A review of circulation dynamics of the coastal oceans near China. *Acta Oceanol. Sin.* 23, 1–16.
- Takahashi, T., Olafsson, J., Goddard, J.G., Chipman, D.W., Sutherland, S.C., 1993. Seasonal variation of CO<sub>2</sub> and nutrients in the high-latitude surface ocean: a comparative study. *Glob. Biogeochem. Cycles* 7, 843–878.
- Takahashi, T., Sutherland, S.C., Wanninkhof, R., Sweeney, C., Feely, R.A., Chipman, D.W., Hales, B., Friederich, G., Chavez, F., Sabine, C., Watson, A., Bakker, D.C.E., Schuster, U., Metzl, N., Yoshikawa-Inoue, H., Ishii, M., Midorikawa, T., Nojiri, Y., Kortzinger, A., Steinhoff, T., Hoppema, M., Olafsson, J., Arnarson, T.S., Tilbrook, B., Johannessen, T., Olsen, A., Bellerby, R., Wong, C.S., Delille, B., Bates, N.R., deBaar, H.J.W., 2009. Climatological mean and decadal change in surface ocean pCO<sub>2</sub>, and net sea–air CO<sub>2</sub> flux over the global oceans. *Deep-Sea Res.* II 56, 554–577.
- Tans, P.P., Fung, I.Y., Takahashi, T., 1990. Observational constraints on the global atmospheric CO<sub>2</sub> budget. *Science* 247, 1431–1438.
- Thomas, H., Bozec, Y., Elkalay, K., de Baar, H.J.W., 2004. Enhanced open ocean storage of CO<sub>2</sub> from shelf sea pumping. *Science* 304. doi:10.1126/science.1095491.
- Tsunogai, S., Watanabe, S., Nakamura, J., Ono, T., Sato, T., 1997. A preliminary study of carbon system in the East China Sea. *J. Oceanogr.* 53, 9–17.
- Tsunogai, S., Watanabe, S., Sato, T., 1999. Is there a “continental shelf pump” for the absorption of atmospheric CO<sub>2</sub>. *Tellus* 51B, 701–712.
- Wang, B., 2006. Cultural eutrophication in the Changjiang (Yangtze River) plume: history and perspective. *Estuar. Coast. Shelf Sci.* 69, 471–477.
- Wang, S.-L., Chen, C.-T.A., Hong, G.-H., Chung, C.-S., 2000. Carbon dioxide and related parameters in the East China Sea. *Cont. Shelf Res.* 20, 525–544.
- Wang, F., Wang, Y., Zhang, J., Xu, H., Wei, X., 2007. Human impact on the historical change of CO<sub>2</sub> degassing flux in River Changjiang. *Geochem. Trans.* 8, 7. doi:10.1186/1467-4866-8-7.
- Wanninkhof, R., 1992. Relationship between wind speed and gas exchange over the ocean. *J. Geophys. Res.* 97 (C5), 7373–7382.
- Wanninkhof, R., Thoning, K., 1993. Measurement of fugacity of CO<sub>2</sub> in surface water using continuous and discrete sampling methods. *Mar. Chem.* 44, 189–204.
- Wei, H., He, Y., Li, Q., Liu, Z., Wang, H., 2007. Summer hypoxia adjacent to the Changjiang Estuary. *J. Mar. Syst.* 67, 292–303.
- Weiss, R.F., 1974. Carbon dioxide in water and seawater: the solubility of a non-ideal gas. *Mar. Chem.* 2, 203–215.
- Weiss, R.F., Price, B.A., 1980. Nitrous oxide solubility in water and seawater. *Mar. Chem.* 8, 347–359.
- Wong, G.T.F., Chao, S.-Y., Li, Y.-H., Shiah, F.-K., 2000. The Kuroshio edge exchange processes (KEEP) study—an introduction to hypotheses and highlights. *Cont. Shelf Res.* 20, 335–347.
- Xie, S., Hafner, J., Tanimoto, Y., Liu, W.T., Tokinaga, H., Xu, H., 2002. Bathymetric effect on the winter sea surface temperature and climate of the Yellow and East China Seas. *Geophys. Res. Lett.* 29, 2228. doi:10.1029/2002GL015884.
- Zhai, W., Dai, M., 2009. On the seasonal variation of air–sea CO<sub>2</sub> fluxes in the outer Changjiang (Yangtze River) Estuary. *East China Sea. Mar. Chem.* 117, 2–10.
- Zhai, W., Dai, M., Guo, X., 2007. Carbonate system and CO<sub>2</sub> degassing fluxes in the inner estuary of Changjiang (Yangtze) River, China. *Mar. Chem.* 107, 342–356.
- Zhang, L., Xue, L., Song, M., Jiang, C., 2010. Distribution of the surface partial pressure of CO<sub>2</sub> in the southern Yellow Sea and its controls. *Cont. Shelf Res.* 30, 293–304.